Line shape of three-level ions in Paul traps

Michael Schubert, Ingo Siemers, and Rainer Blatt
I. Institut für Experimentalphysik, Jungiusstrasse 9, D-2000 Hamburg, Federal Republic of Germany
(Received 5 December 1988)

A cloud of three-level ions (Ba^+) confined in a Paul trap was illuminated with two lasers and the resulting fluorescence was observed as a function of the laser detunings from the ionic resonance. The observed spectra show features due to the oscillatory motion of the trapped ions. In order to describe the observed line shapes, calculations are presented in which the ion ensemble is separated in classes of velocity amplitudes of the oscillatory motion rather than velocity classes.

I. INTRODUCTION

Ion traps provide a tool which allows one to store ions for long times[1] without perturbations by collisions with confining walls. Long interaction times between the ions and externally applied fields are possible, and spectra can be obtained without transit-time broadening or collisional influences. Hence, the ion-storage technique is ideally suited for high-precision measurements, and consequently its application for time and frequency standards has been both proposed and investigated.[2] Currently, the largest remaining systematic error in the determination of center frequencies of spectral lines is given by the Doppler effect. In the microwave domain first-order Doppler effects can be overcome by confining the ions to dimensions smaller than the transition wavelength (Dicke criterion). This allowed, for example, ultrahigh-precision measurements of hyperfine separations,[3] where the accuracy is generally limited by the second-order Doppler effect. More recently, increasing interest has been devoted to the spectroscopy of trapped ions in the optical domain, too as, e.g., the measurements of lifetimes of metastable states and isotopic shifts.[4,5] In the optical region, however, the ion motion results in a broadening of the observed line shapes due to the first-order Doppler effect.

In principle, this limitation could be overcome by the application of laser cooling. Unfortunately, it turned out that laser cooling of trapped ions is efficient only for very small ion clouds (a few tens of ions) due to an effect commonly known as rf heating.[6] Of course, spectroscopic experiments on single cooled ions have been demonstrated[7] and seem to be the ultimate tool for ultrahigh-precision experiments. However, many spectroscopic investigations (as, e.g., lifetime and branching ratio measurements, isotopic shifts, etc.[5,8] are much easier performed on clouds of trapped ions when utmost precision is not required. Nevertheless, for these experiments, a thorough and detailed understanding of the line shapes of trapped ions is certainly desirable.

The line shape, i.e., the dependence of the occupation probability of the fluorescing state on the detuning of the frequencies of the applied laser fields from the ionic resonances, is usually calculated by assuming velocities as constants during the measurement process. That is to say, atom (or ion) ensembles are considered to be separated into velocity classes. For each velocity class the occupation probability of the fluorescing state is computed using time-independent steady-state theory, which is then convoluted with the ensemble's velocity distribution to obtain the line shape. Such an approach is certainly valid for atoms in a gas; their velocity is constant between successive collisions, the rate of which can be made smaller than the spontaneous decay rate of a dipole-allowed transition.

In ion traps, however, things are different. Traps, by definition, make use of a potential which exerts a restoring force upon particles that have left the equilibrium point. Thus in any trap the motion of trapped particles is oscillatory. In Paul traps there is a second source of oscillatory motion, since the confining potential is generated by an rf modulation of the ions' velocities.[6] Therefore, in an ion's rest frame of reference, a laser field appears frequency modulated. Its spectrum consists of an unshifted carrier and sidebands. This form of the light field has a profound influence on the line shape, as will be outlined in this paper. In order to do so, only simple oscillatory motion will be considered. All ions are assumed to oscillate with the same frequency, but with different velocity amplitudes $\bar{v}$. Therefore each ion is labelled by its velocity amplitude rather than its velocity $v(t)$, i.e., the ion ensemble is separated into velocity amplitude classes $\bar{v}$ instead of velocity classes v.

In Sec. II A we review the theory of the ionic motion in Paul traps.[6,9,10] The line shape is calculated in Sec. II B for a single harmonically oscillating ion of a given velocity amplitude. Its density matrix is written as a Fourier series whose coefficients are given in terms of matrix continued fractions. The line shape for an ensemble of ions is then calculated by convoluting the results for one ion of given velocity amplitude with the distribution of velocity amplitudes. In Sec. III the calculated line shapes are compared with measurements made on clouds of Ba^+ ions in Paul traps.

II. THEORY OF THE LINE SHAPE

A. Ion motion in Paul traps

Trapping of charged particles in Paul traps (rf quadrupole traps) is achieved by means of the time-dependent potential

$$\Phi(r,z,t)=-\frac{m\Omega^2}{16e}[a_z-2q_z\cos(\Omega t)](r^2-2z^2)\ , \tag{1}$$

with $r^2=x^2+y^2$ and

$$a_z=-2a_r=-\frac{8eU}{mr_0^2\Omega^2},\quad q_z=-2q_r=\frac{4eV}{mr_0^2\Omega^2}\ ,$$

as has been described by many authors.[6,9,10] x,y,z denote the axes of a Cartesian coordinate system, e is the elementary charge (assuming ions with single positive charge), m is the mass of the ion, r_0 is the radius of the trap's ring electrode, $z_0=r_0/\sqrt{2}$ is half the distance of the trap's end caps, U and V are the applied dc and ac voltages, respectively, and $\Omega/2\pi$ is the driving frequency of the trap. Ponderomotive forces due to the time-dependent potential determine the secular frequencies of the ion motion $\omega_i=\beta_i\Omega/2$ $(i=r,z)$ with $\beta_i=\beta_i(a_i,q_i)$. Supposed on this secular motion (macromotion) is the oscillating motion at the trap's driving frequency Ω (micromotion).

In order to determine the line shapes for spectroscopic experiments, usually velocity distributions are exploited. The dynamics of ion clouds in Paul traps has been described recently in the frame of a Brownian motion model yielding the velocity distribution of the ion cloud:

$$P(v,t)=\frac{1}{(2\pi)^{1/2}\sigma(t)}\exp\left[-\frac{v^2}{2\sigma^2(t)}\right]\ . \tag{2}$$

This Gaussian distribution contains a time-dependent variance $\sigma(t)$, i.e., its width varies periodically with the driving frequency Ω. Details of the calculation of the mean-squared velocity $\sigma(t)$ have been given in Ref. 11.

The usual procedure of calculating line shapes would be to compute the steady-state solution for the occupation probability of the fluorescing state and to convolute it with its velocity distribution [Eq. (2)]. Figure 1 shows a Λ-type three-level system as is approximately realized with Ba^+ ions, which have been used in experiments with trapped ion clouds.[12] The transitions $|1\rangle\rightleftarrows|2\rangle$, $|3\rangle\rightleftarrows|2\rangle$ are dipole allowed; state $|3\rangle$ is assumed to be metastable. In the case of Ba^+ the measured lifetime of the $^2D_{3/2}$ level is 17 s.[4] Fluorescence is observed on the transition $|1\rangle\rightleftarrows|2\rangle$. In order to keep a steady flux of fluorescence, a second laser is required on the transition $|3\rangle\rightleftarrows|2\rangle$, thus preventing optical pumping to state $|3\rangle$. The interaction of the two light fields at 493 and 650 nm with the ion is described in dipole approximation by their Rabi frequencies Ω_r,Ω_g (r, 650 nm; g, 493 nm) and the detunings Δ_r,Δ_g, respectively. The detunings are defined as $\omega_{\text{laser}}-\omega_{\text{ion}}$. The **k** vectors of the light fields can be chosen to be collinear or anticollinear. According to the usual method the observed line shape $L(\Delta_g)$ would be given by

$$L(\Delta_g)=\int_{-\infty}^{\infty}\overline{P(v,t)}\rho_{22}(\Delta_g-k_gv,\Delta_r-k_rv)dv\ , \tag{3}$$

$\overline{P(v,t)}$ being the time average of the distribution of velocities [Eq. (2)]. Here $\rho_{22}(\ )$ is the density matrix element describing the occupation probability of state $|2\rangle$ as a function of the laser detunings Δ_g,Δ_r and the velocity-induced Doppler shifts k_gv,k_rv.

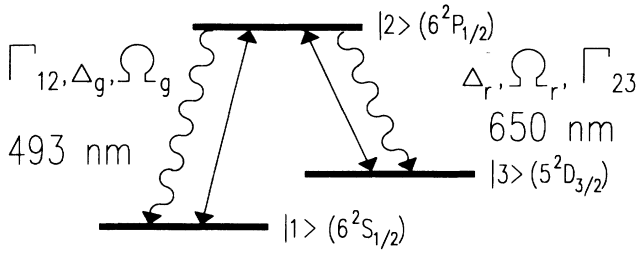

FIG. 1. Relevant energy levels of the Ba^+ ion.

This calculation yields a line shape as shown in Fig. 2 (parameters: $\Delta_r=0$, collinear laser beams, mean width $\sigma=1000$ m/s). Two features are worth noting.

First, it has a doubly peaked structure with the minimum resulting from a coherent superposition of states $|1\rangle$ and $|3\rangle$. Such a coherent superposition does not interact with the exciting light fields if its internal phase differs from the phase difference of both light fields by π. Moreover, the decay of the superposition is only determined by the decay time of the metastable state $|3\rangle$ because the ground state is stable. Hence occupation in the coherent superposition state accumulates, and ρ_{22} is subsequently reduced [(Ref. 13), "dark resonance," "nonabsorption resonance"]. This dip has reduced Doppler width, since the first-order Doppler shifts of the two lasers subtract, $(k_g-k_r)v$.

Second, the calculated width of the line of ≈ 300 MHz [full width at half maximum (FWHM)] is much smaller than the Doppler width $2k_g\sigma\approx 4$ GHz. The reason is that the width of the line is determined by the necessity that *both* laser frequencies coincide with the ionic transition frequencies within a width given by the degree of saturation and the natural linewidth in order to provide

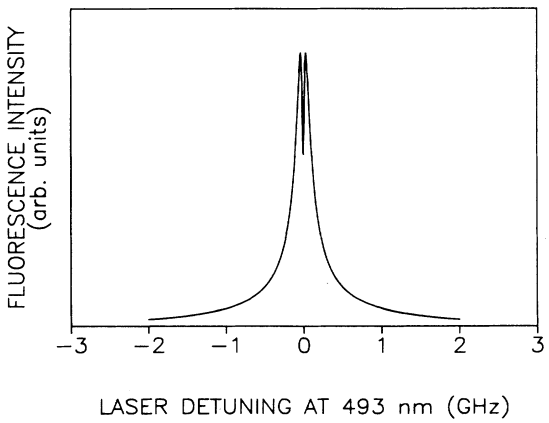

FIG. 2. Line shape of the ion cloud as calculated from the velocity class model [Eq. (3)]. Though the mean-squared velocity is 1000 m/s, the linewidth is only approximately 300 MHz (FWHM), due to cross saturation.

sufficient occupation in the state $|2\rangle$ (similar to cross saturation[14]). This can be achieved only for a few velocity classes. As a consequence, the linewidth does not depend on the width σ of the velocity distribution as long as $k_g\sigma$ is much larger than the saturation broadened, natural line width of the ionic transition. Thus linewidths larger than $\approx$300 MHz cannot be explained in this frame. However, the experimentally observed linewidth is about several GHz (Ref. 12, see Fig. 7). Obviously, the calculation is inconsistent with the experimental data. This led to a detailed calculation of the line shape of a Λ-type three-level system with particular consideration of the oscillatory motion of trapped ions.

B. Line-shape calculation

In order to calculate the line shape of trapped ions, their motion must be known since it enters the problem through the Doppler effect. The motion of a single trapped ion is determined by the trap's potential [Eq. (1)] and the initial conditions. In the presence of other ions their mutual repulsive Coulomb interaction has to be taken into account. This results in a fairly complicated structure of the ions' motion. However, it has one characteristic feature: It is oscillatory. Hence, as a first approximation, we consider only harmonic oscillation. There are two natural choices for the oscillation frequency of the ions, the trap's driving frequency Ω, and the secular frequencies ω_r,ω_z (which one, depends on the orientation of the **k** vectors of the light fields relative to the trap's axis). Since there is negligible dependence of the results on the choice of the oscillation frequency (see below), we have used the trap's driving frequency Ω throughout this paper. Hence we write for the ion's velocity

$$v(t)=\bar{v}\cos(\Omega t)\ , \tag{4}$$

where $\bar{v}$ denotes the velocity amplitude of the ion's motion. Thus in the ion's rest frame of reference the laser fields can be written as

$$\mathbf{E}=\mathbf{E}_g\cos\left[\omega_{\text{laser,green}}t-\frac{k_g\bar{v}}{\Omega}\sin(\Omega t)\right]+\mathbf{E}_r\cos\left[\omega_{\text{laser,red}}t-\frac{k_r\bar{v}}{\Omega}\sin(\Omega t)\right]\ .$$

The spectrum of these fields contains the carrier frequencies $\omega_{\text{laser,red}},\omega_{\text{laser,green}}$ and equidistant sidebands spaced by Ω. The number of sidebands is approximately given by the modulation indices $\mu_r=k_r\bar{v}/\Omega$, $\mu_g=k_g\bar{v}/\Omega$, so the sidebands extend over a range of $2\mu_g\Omega=2k_g\bar{v}$ (analogous to the red laser). For parameters as in the experiments described below, i.e., $\Omega/2\pi=500$ kHz and $\bar{v}=1000$ m/s, we compute $\mu_g\approx4000$. The relative intensity of the nth sideband is given by $|J_n(\mu)|^2$, $J_n(\mu)$ being the nth-order Bessel function. Note that the ionic frequencies Ω, ω_r, and ω_z are smaller than the radiative linewidths of the driven transitions of the ion. This explains why the results of the calculations show negligible dependence on the choice of Ω or ω_r,ω_z as oscillation frequency in Eq. (4).

The internal degrees of freedom of a three-level atom are described by its 3×3 density matrix ρ which obeys the equation

$$i\hbar\frac{d}{dt}\rho=[H,\rho]+\text{relaxation terms}\ .$$

Using the rotating wave approximation, the set of differential equations reads explicitly[13]

$$\begin{aligned}
\dot{\rho}_{11}&=\Omega_g\mathrm{Im}\rho_{12}+\Gamma_{12}(1-\rho_{11}-\rho_{33})+2\gamma_{13}\rho_{33}\ ,\\
\dot{\rho}_{33}&=\Omega_r\mathrm{Im}\rho_{32}+\Gamma_{32}(1-\rho_{11}-\rho_{33})-2\gamma_{13}\rho_{33}\ ,\\
\mathrm{Im}\dot{\rho}_{12}&=-[\Delta_g-k_g\bar{v}\cos(\Omega t)]\mathrm{Re}\rho_{12}-\gamma_{12}\mathrm{Im}\rho_{12}\\
&\quad-\Omega_g(2\rho_{11}+\rho_{33}-1)/2-\Omega_r\mathrm{Re}\rho_{13}/2\ ,\\
\mathrm{Re}\dot{\rho}_{12}&=[\Delta_g-k_g\bar{v}\cos(\Omega t)]\mathrm{Im}\rho_{12}-\gamma_{12}\mathrm{Re}\rho_{12}+\Omega_r\mathrm{Im}\rho_{13}/2\ ,\\
\mathrm{Im}\dot{\rho}_{32}&=-[\Delta_r-k_r\bar{v}\cos(\Omega t)]\mathrm{Re}\rho_{32}-\gamma_{32}\mathrm{Im}\rho_{32}\\
&\quad-\Omega_r(2\rho_{33}+\rho_{11}-1)/2-\Omega_g\mathrm{Re}\rho_{13}/2\ ,\\
\mathrm{Re}\dot{\rho}_{32}&=[\Delta_r-k_r\bar{v}\cos(\Omega t)]\mathrm{Im}\rho_{32}-\gamma_{32}\mathrm{Re}\rho_{32}-\Omega_g\mathrm{Im}\rho_{13}/2\ ,\\
\mathrm{Im}\dot{\rho}_{13}&=-[\Delta_g-\Delta_r-(k_g-k_r)\bar{v}\cos(\Omega t)]\mathrm{Re}\rho_{13}-\gamma_{13}\mathrm{Im}\rho_{13}\\
&\quad+\Omega_g\mathrm{Re}\rho_{32}/2-\Omega_r\mathrm{Re}\rho_{12}/2\ ,\\
\mathrm{Re}\dot{\rho}_{13}&=[\Delta_g-\Delta_r-(k_g-k_r)\bar{v}\cos(\Omega t)]\mathrm{Im}\rho_{13}-\gamma_{13}\mathrm{Re}\rho_{13}\\
&\quad+\Omega_g\mathrm{Im}\rho_{32}/2+\Omega_r\mathrm{Im}\rho_{12}/2\ ,\\
\dot{\rho}_{22}&=-\dot{\rho}_{11}-\dot{\rho}_{33}\ .
\end{aligned}$$

Here, Γ_{12} and Γ_{32} are the decay rates of the population of the state $|2\rangle$ to the levels $|1\rangle$ and $|3\rangle$, respectively. Further, $2\gamma_{12}=\Gamma_{12}$, $2\gamma_{32}=\Gamma_{32}+2\gamma_{13}$. In order to arrive at these equations, ρ_{22} was eliminated using $\mathrm{tr}\rho=1$, and rapidly oscillating terms in the coherences $\rho_{12},\rho_{32},\rho_{13}$ have been transformed out. The detunings are defined as

$$\Delta_r=\omega_{\text{laser,red}}-\omega_{23},\quad \Delta_g=\omega_{\text{laser,green}}-\omega_{21}\ .$$

This set of equations is a linear inhomogeneous system of eight differential equations with periodic coefficients for the vector $\boldsymbol{\rho}$,

$$\boldsymbol{\rho}=(\rho_{11},\rho_{33},\mathrm{Im}\rho_{12},\mathrm{Re}\rho_{12},\mathrm{Im}\rho_{32},\mathrm{Re}\rho_{32},\mathrm{Im}\rho_{13},\mathrm{Re}\rho_{13})\ ,$$

which can be written more explicitly as

$$\frac{d}{dt}\boldsymbol{\rho}=[A+2B\cos(\Omega t)]\boldsymbol{\rho}+\boldsymbol{\mu}\ . \tag{5}$$

A and B denote constant, real-valued 8×8 matrices and are given explicitly in the Appendix. We obtain for the vector $\boldsymbol{\mu}$

$$\boldsymbol{\mu}=(\Gamma_{12},\Gamma_{32},\Omega_g/2,0,\Omega_r/2,0,0,0)\ .$$

The damping constants in these equations lead to the existence of a quasistationary solution in the long-time limit. In this case, which is the only one investigated in this paper, $\boldsymbol{\rho}(t)$ is periodic with period $2\pi/\Omega$,

$$\rho(t)=\sum_{m=-\infty}^{\infty}\rho_m e^{-im\Omega t}\ .$$

Inserting this into the Liouville equation (5) leads to a recurrence relation for the Fourier coefficients ρ_n,

$$(A+in\Omega)\rho_n+B(\rho_{n+1}+\rho_{n-1})+\mu\delta_{n0}=0\ .$$

The solution of this tridiagonal recurrence relation has been shown to be[15]

$$\rho_0=-(A+2B\ \mathrm{Re}S_0^+)^{-1}\mu$$

with the matrix S_0^+ determined by the matrix continued fraction

$$S_{n-1}^+=-(A+in\Omega+BS_n^+)^{-1}B$$

which has to be evaluated numerically. This method has also been used by Javanainen[16] to calculate the light force on a harmonically oscillating three-level ion.

In the following, the values Ω_r,Ω_g are kept fixed at $\Omega_r=5\Gamma_{32}$, $\Omega_g=\Gamma_{12}$. These values correspond to the intensities used in the experiment described below. $\Gamma_{12}/2\pi=15.1$ MHz, $\Gamma_{32}/2\pi=5.3$ MHz, $2\gamma_{13}=1/17\ \mathrm{s}^{-1}$, these values correspond to the Ba^+ ion. The observed fluorescence in the experiment is given by the time average of $\Gamma_{12}\rho_{22}$; therefore ρ_{22} is of particular interest for the line-shape calculations. The frequency Ω is $2\pi\times500$ kHz.

Figure 3(a) shows the time average of $\rho_{22}(t)$ of one harmonically oscillating ion as a function of Δ_g (collinear laser beams, $\bar{v}=300$ m/s, $\Delta_r=-300$ MHz). The state $|2\rangle$ is occupied for all detunings Δ_g with $-k_g\bar{v}\le\Delta_g\le k_g\bar{v}$. At $\Delta_g\approx-400$ MHz there is a dip in the occupation probability which is due to a coherent superposition of states $|1\rangle$ and $|3\rangle$, as already encountered in Sec. II A. Except for this dark resonance between the two peaks [of Fig. 3(a)], $\overline{\rho_{22}(t)}$ (the bar denotes the time average over one period of the trap's driving field) reminds one of the form of the velocity distribution of a harmonic oscillator

$$\frac{1}{[(k_g\bar{v})^2-\Delta_g^2]^{1/2}}\ . \tag{6}$$

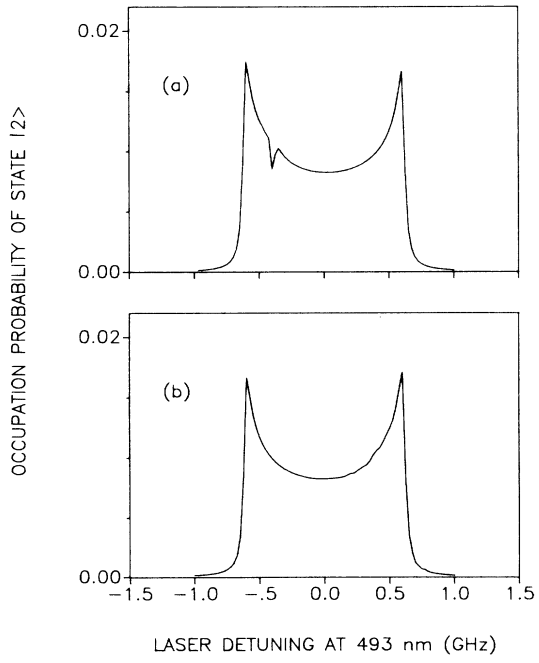

FIG. 3. Time-averaged occupation probability $\overline{\rho_{22}(t)}$ of state $|2\rangle$ for a single harmonically oscillating ion of velocity amplitude $\bar{v}=300$ m/s, as a function of the detuning of the laser at 493 nm. The detuning at 650 nm is $\Delta_r=-300$ MHz; the laser beams are collinear (a), anticollinear (b).

Figure 3(b) shows $\overline{\rho_{22}(t)}$ for the same parameters as in Fig. 3(a) ($\Delta_r=-300$ MHz, $\bar{v}=300$ m/s), but for anticollinear laser beams. The result is very similar except for the appearance of the dark resonance. Here it does not occur because the Doppler shifts of the two lasers add $[(k_r+k_g)v]$ and broaden the dark resonance. In the case of collinear beams, the Doppler shifts subtract $[(k_r-k_g)v]$ and the dark resonance has reduced Doppler width.[13]

To obtain the line shape of an ensemble of ions, the result for a particular velocity amplitude class has to be convoluted with the distribution of velocity amplitudes. The velocity distribution itself takes the form of a Gaussian with width σ [Eq. (2)], which for simplicity we take to be constant in time. The implications of this approximation have been discussed in Ref. 12. It could be circumvented by lengthy numerical work. Recalling the velocity distribution of the ion cloud [Eq. (2)] and the velocity distribution of a velocity amplitude class [Eq. (6)], we realize that the distribution of velocity amplitudes $F(\bar{v})$ has to fulfill the relation

$$\frac{1}{\sqrt{2\pi}\sigma}\exp\left[-\frac{v^2}{2\sigma^2}\right]=\int_v^\infty\frac{F(\bar{v})d\bar{v}}{\pi(\bar{v}^2-v^2)^{1/2}}\ . \tag{7}$$

Thus we assume that the cloud's velocity distribution is built up from an ensemble of harmonic oscillators. As a solution to Eq. (7) we find

$$F(\bar{v})=\bar{v}\sigma^{-2}\exp\left[-\frac{\bar{v}^2}{2\sigma^2}\right]\ .$$

The line shape $L(\Delta_g)$ is then given by

$$L(\Delta_g)=\int_0^\infty F(\bar{v})\rho_{22}(\bar{v},\Delta_g)d\bar{v}\ . \tag{8}$$

According to this procedure $L(\Delta_g)$ was calculated for $\Delta_r=0$, $\sigma=500$ m/s (collinear beams) and is displayed in Fig. 4. It has a width equal to $k_g\sigma$ which reflects the width of the underlying velocity distribution. Thus, the mean kinetic energy of the ion cloud can be determined from a measurement of the width of the line shape as has been done previously.[12] Note that in spite of the involved line-shape calculations the kinetic energy can be extracted from measured line shapes without difficulty.

We would like to emphasize that this result is not expected if one strictly argues on the basis of velocity classes as it is usually done in spectroscopic line-shape

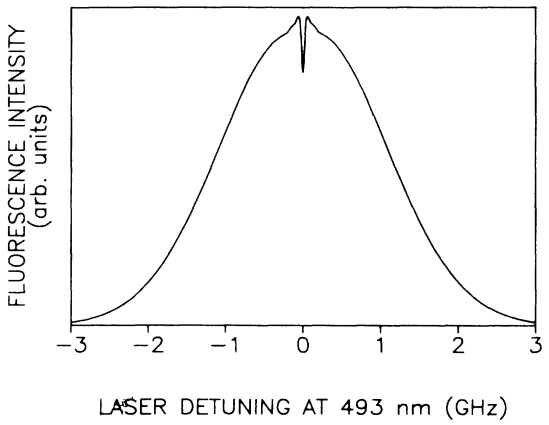

FIG. 4. Line shape of the ion cloud as calculated from Eq. (8). The mean-squared velocity is 500 m/s, and $\Delta_r=0$ (collinear laser beams).

calculations. Taking that point of view for the moment, one reasons that an ion of a particular velocity class has to be in resonance with *both* lasers in order to fluoresce. This infers two conditions which select *one* velocity class (in fact, due to the natural line width of the ionic transition and the degree of saturation, a small group of velocity classes is selected). Thus the resulting line shape is expected to have sub-Doppler width, as is intentionally the case in cross-saturation spectroscopy.[14] This is in contradiction with the result displayed in Fig. 4, which has full Doppler width. We conclude that the oscillatory motion of trapped ions destroys the cross saturation and results in a line shape displaying full Doppler width even in a three-level system interacting simultaneously with two lasers. Inspection of the line shape in the case of anticollinear beams shows the same form as in the collinear case except for the dark-resonance dip which does not show up.

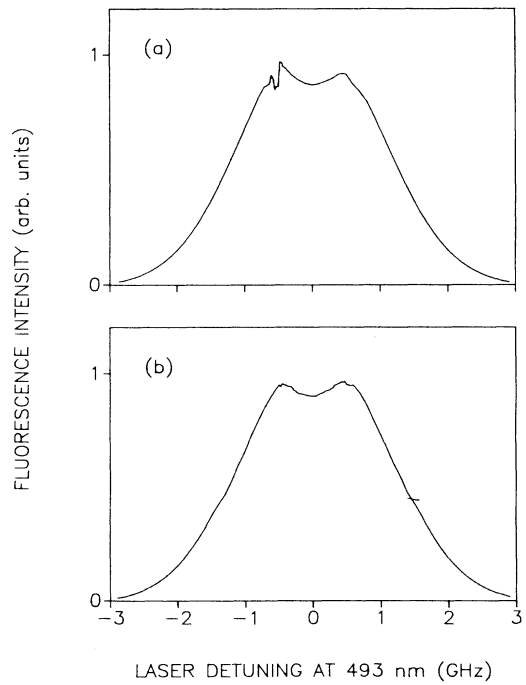

FIG. 5. Line shape of the ion cloud [Eq. (8)] for detuned red laser ($\Delta_r=-400$ MHz); $\sigma=500$ m/s. The laser beams are collinear (a), anticollinear (b).

The line shape $L(\Delta_g)$ has been investigated for the case $\Delta_r\neq 0$, too. Figure 5(a) shows $L(\Delta_g)$ for $\Delta_r=-400$ MHz, $\sigma=500$ m/s, and collinear laser beams; Fig. 5(b) displays the result for the same parameters but anticollinear beams. Both figures show a modification of the line center as compared to Fig. 4. The reason for this can be understood as follows: In the rest frame of an ion of velocity amplitude class $\bar{v}$ the light field at the transition $|2\rangle\rightleftarrows|3\rangle$ has sidebands ranging from $\Delta_r-k_r\bar{v}$ to $\Delta_r+k_r\bar{v}$. If $\bar{v}<|\Delta_r|/k_r$, none of these sidebands will be resonant with the ionic transition and the ion will not fluoresce much. If, on the contrary, $\bar{v}>|\Delta_r|/k_r$, some sideband will be resonant, and the ion will be able to fluoresence. Thus, an ion needs a minimum velocity amplitude $\bar{v}=|\Delta_r|/k_r$ to show some fluorescence light. Consequently, the fluorescence of ions with small velocity amplitudes is missing in the line shape calculated for $\Delta_r\neq 0$. It lacks some fluorescence in the region

$$-|\Delta_r|k_g/k_r<\Delta_g<|\Delta_r|k_g/k_r\ .$$

This is immediately recognized in Fig. 5(b) showing the anticollinear case. Figure 5(a) shows essentially the same feature (flattened top of line shape) but its interpretation is a little more involved, and the appearance is slightly obscured by the presence of the (almost Doppler-free) dark resonance (indicated by the little dip left of the flattened top). To summarize, the physical basis of the lineshape interpretation is optical pumping of those ions whose velocity amplitudes are not large enough to reach the velocity amplitude determined by the detuning $\Delta_r\neq 0$.

All calculations have been performed by assuming an ion oscillating at the trap's driving frequency Ω. One could also choose one of the secular frequencies ω_r,ω_z as oscillation frequency. Because the arguments used exploit only the structure of the light fields in the ion's rest frame of reference (frequency-modulated laser fields) and the kinetic energy in both macro- and micromotion is of the same order of magnitude, no change of the results is expected. Both the dark resonance in the collinear case and the flattened top in the case $\Delta_r\neq 0$ show up in calculations carried out with ω_r,ω_z as oscillation frequency. Judging from the form of the line shape alone, there is no way to distinguish influences of micro- and macromotion.

III. EXPERIMENTAL DETERMINATION OF THE LINE SHAPE

The experimental setup is schematically given in Fig. 6. The light field at 493 nm is generated by a cw ring dye laser which excites the ionic transition $6\,^2S_{1/2}\rightleftarrows 6\,^2P_{1/2}$. The $6\,^2P_{1/2}$ state decays to the states $6\,^2S_{1/2}$ and $5\,^2D_{3/2}$ with a branching ratio of 3:1. In order to prevent optical

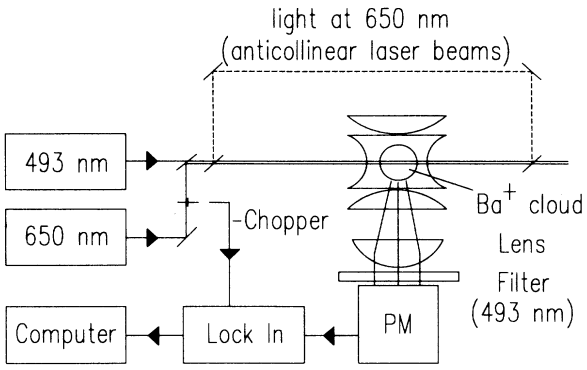

FIG. 6. Experimental setup for the measurement of the line shapes of clouds of trapped Ba^+ ions.

pumping to the $5\,^2D_{3/2}$ state [this state has a lifetime of 17 s (Ref. 4)], a second laser at 650 nm is necessary. Both lasers propagate through the ring plane of the rf trap (ring diameter 40 mm), either collinearly or anticollinearly. Fluorescence at 493 nm is observed at a right angle to the laser beams through one of the end caps formed of a mesh and is detected by a photomultiplier (PM). For lock-in detection, the laser at 650 nm is periodically chopped, which results in a clear signal at 493 nm since there is immediate optical pumping to the $5\,^2D_{3/2}$ state when no radiation at 650 nm is present. The line shape is obtained by recording the photomultiplier current as a function of the detuning of the laser at 493 nm.

The atomic beam, from which the ions are created by electron impact ionization, is blocked by a mechanical beam shutter during the measurements. The background pressure inside the trap is about 10^{-6} Pa.

Figure 7 shows a measurement for $\Delta_r=0$ and collinear beams; Fig. 8 one for $\Delta_r=0$ and anticollinear beams. As predicted, the line shapes have widths of several GHz and are not Doppler free as would be expected for cross

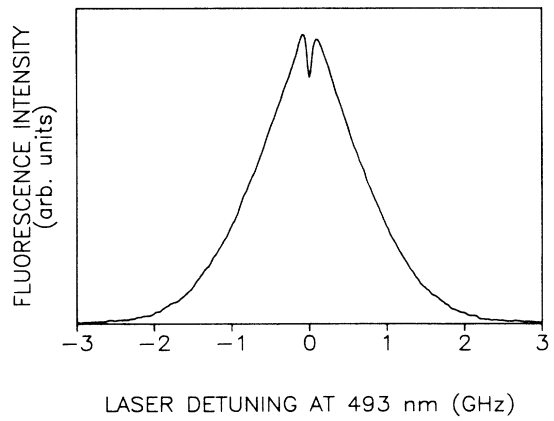

FIG. 7. Experimentally observed line shape of the ion cloud ($\Delta_r=0$) for collinear beams.

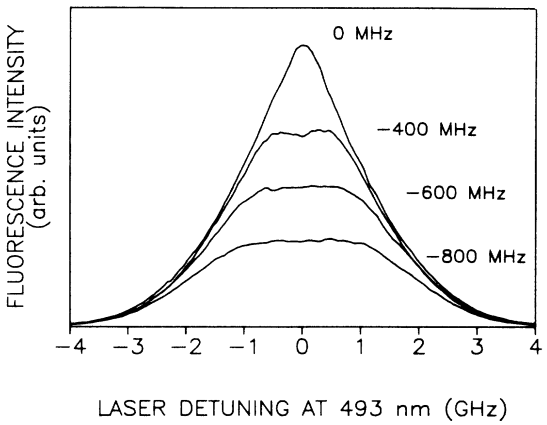

FIG. 8. Measured line shapes for several detunings Δ_r of the laser at 650 nm (anticollinear beams).

saturation. In particular, the line shapes do not display the form calculated on the basis of velocity classes (Fig. 2). The cross saturation is destroyed by the frequency modulation of the light fields. The dark resonance shows up in the collinear case, but not in the anticollinear one.

Figure 8 shows the observed line shapes for anticollinear beams and several detunings of the laser at 650 nm. The line shapes approximately coincide in the wings but differ in the center, where their top is flattened. One could imagine that they arise from the line shape for $\Delta_r=0$ by cutting it horizontally in a certain height depending on the detuning of the light field at 650 nm. The widths of the flat areas depend linearly on the absolute value of the detuning at 650 nm. This confirms the interpretation given in Sec. II B, stating that ions need a minimum velocity amplitude $\tilde{v}=|\Delta_r|/k_r$ in order to fluoresce. Conversely, fluorescence light of the ions with velocity amplitude $\tilde{v}\leq|\Delta_r|/k_r$ is missing in the line center, since they are optically pumped to the $5\,^2D_{3/2}$ state. Note that the experimental results of Fig. 8 and the calculated line shape of Fig. 5(b) most clearly demonstrate the suitability of the concept of separation of the ion ensemble into classes of velocity amplitude rather than velocity. The flattened tops of the spectra can be easily understood as arising from optical pumping of certain velocity amplitude classes. Of course, every velocity amplitude class can be considered to consist of many velocity classes, Eq. (6), and vice versa, so an interpretation in terms of velocity classes is in principle possible but very complicated. Moreover, it would obscure the underlying physical processes instead of clarifying them. We conclude that the concept of velocity amplitude classes is well suited for the understanding of line shapes measured on clouds of trapped ions.

Figure 9 shows the observed line shape for collinear beams and a detuning $\Delta_r=-400$ MHz. As in the previous case, fluorescence is reduced in the central region. Due to the occurrence of the dark resonance left of the flattened top, the line shape is modified in agreement with the theoretical prediction [cf. Fig. 5(a)].

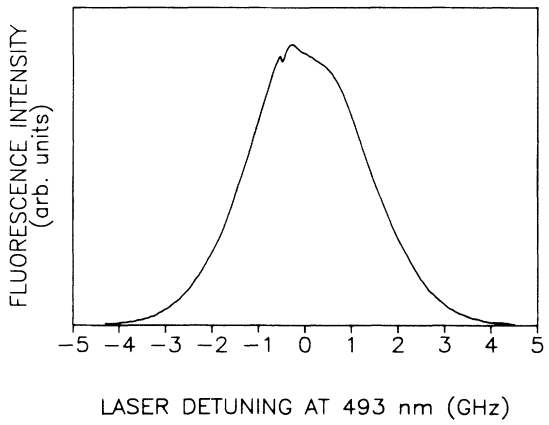

FIG. 9. Measured line shape for $\Delta_r = -400$ MHz, collinear beams.

IV. CONCLUSIONS

It has been demonstrated both theoretically and experimentally that the oscillatory motion of trapped ions strongly influences the observed line shapes in spectroscopic experiments. The calculations and measurements agree qualitatively in general. Additionally, separating the ion ensemble into velocity amplitude classes gives an intuitive physical picture that accounts for the processes of optical pumping encountered in the case of nonresonant laser tuning. Moreover, two-photon processes lead to the dark resonance. We conclude that it seems necessary to describe the ion motion in terms of velocity amplitudes instead of velocities themselves. It should be mentioned that arguments based on velocity amplitudes have been used previously in order to explain observed line shapes in clouds of trapped ions.[17]

Our calculations predict that the line shapes for $\Delta_r = 0$ have full Doppler width. Thus the mean kinetic energy of the ion cloud can be determined from such a measurement.[12] The knowledge of the mean kinetic energies of the ion cloud is important for frequency standards applications of spectroscopic measurements, e.g., the correction of second-order Doppler shifts of hyperfine splittings. In these experiments, line centers are shifted because of the second-order Doppler effect which is proportional to the ion cloud's mean kinetic energy. Such shifts can be corrected for if the ion's energy is known.

The calculations can be applied to two-level atoms as well. In this case the line shape of an ion ensemble is identical to the line shape derived on the assumption of a separation into velocity classes, at least in the case of large Doppler width. This remark, however, does not invalidate the notion of velocity amplitude classes, since in the ion's rest frame of reference the laser field is not frequency shifted but frequency modulated. This should be observable in experiments based on the selection of certain velocity classes with velocities not equal to zero.

Measurements of the time dependence of the ions' fluorescence, e.g., on time scales of the trap frequency Ω, are difficult to interpret. No doubt, the calculation gives all Fourier coefficients ρ_n of the density matrix, but except ρ_0 they are sensitively dependent on the exact form of $v(t)$. In reality $v(t)$ is not of simple harmonic time dependence, and, because of space charge, it does not vary according to a solution of the Mathieu equation governing the motion of a single ion in the trap potential either. Thus there seems to be no obvious way to improve the given calculations.

It should be possible to successfully apply these calculations to spatially resolved measurements of the ion cloud's fluorescence. Since the Brownian motion model[11] of ion motion in an rf trap predicts a correlation between position and velocity, it should be possible to obtain the spatial distribution of velocity amplitudes, too. As the form of the line shape turned out to be different from the form of the velocity distribution in general in this paper (see Figs. 8 and 9), in the spatially resolved case the spatial distribution of fluorescence should be different from the spatial distribution of the ions themselves.

As has been pointed out, the choice between the trap's driving frequency Ω and the secular frequencies ω_r, ω_z as ionic oscillation frequency cannot be made on the basis of the line shapes alone. Since the micro- and macromotion have different spatial dependence, spatially resolved measurements should shed some light on this question. An investigation of the spatial dependence of the ions' fluorescence will be presented in a forthcoming paper.

ACKNOWLEDGMENTS

We gratefully acknowledge continuous support by Professor P. E. Toschek and Professor W. Neuhauser, and thank them for many stimulating discussions. This work was supported by the Deutsche Forschungsgemeinschaft. One of us (I.S.) thanks the Claussen-Stiftung for additional support.

APPENDIX

Here we present matrices A and B that occur in Eq. (5):

$$A = \begin{pmatrix} -\Gamma_{12} & -\Gamma_{12}+2\gamma_{13} & \Omega_g & 0 & 0 & 0 & 0 & 0 \\ -\Gamma_{23} & -\Gamma_{23}-2\gamma_{13} & 0 & 0 & \Omega_r & 0 & 0 & 0 \\ -\Omega_g & -\Omega_g/2 & -\gamma_{12} & -\Delta_g & 0 & 0 & 0 & -\Omega_r/2 \\ 0 & 0 & \Delta_g & -\gamma_{12} & 0 & 0 & \Omega_r/2 & 0 \\ -\Omega_r/2 & -\Omega_r & 0 & 0 & -\gamma_{32} & -\Delta_r & 0 & -\Omega_g/2 \\ 0 & 0 & 0 & 0 & \Delta_r & -\gamma_{32} & -\Omega_g/2 & 0 \\ 0 & 0 & 0 & -\Omega_r/2 & 0 & \Omega_g/2 & -\gamma_{13} & -(\Delta_g-\Delta_r) \\ 0 & 0 & \Omega_r/2 & 0 & \Omega_g/2 & 0 & (\Delta_g-\Delta_r) & -\gamma_{13} \end{pmatrix},$$

$$B=\begin{bmatrix} 0 & 0 & 0 & 0 & 0 & 0 & 0 & 0 \\ 0 & 0 & 0 & 0 & 0 & 0 & 0 & 0 \\ 0 & 0 & 0 & k_g\bar{v}/2 & 0 & 0 & 0 & 0 \\ 0 & 0 & -k_g\bar{v}/2 & 0 & 0 & 0 & 0 & 0 \\ 0 & 0 & 0 & 0 & 0 & k_r\bar{v}/2 & 0 & 0 \\ 0 & 0 & 0 & 0 & -k_r\bar{v}/2 & 0 & 0 & 0 \\ 0 & 0 & 0 & 0 & 0 & 0 & 0 & (k_g-k_r)\bar{v}/2 \\ 0 & 0 & 0 & 0 & 0 & 0 & -(k_g-k_r)\bar{v}/2 & 0 \end{bmatrix}.$$

[1]H. Dehmelt, in *Advances in Laser Spectroscopy,* Vol. 95 of *NATO ASI Series B: Physics,* edited by F. T. Arecchi, F. Strumia, and H. Walther (Plenum, New York, 1983).

[2]H. Dehmelt, IEEE Trans. Instrum. Meas. **IM-31**, 83 (1982); P. E. Toschek, in *New Trends in Atomic Physics,* Proceedings of Les Houches Session 38, edited by G. Grynberg and R. Stora (North-Holland, Amsterdam, 1984), Vol. 1, p. 381; G. Werth, Metrologia **22**, 190 (1986); D. J. Wineland, Proc. IEEE **74**, 147 (1986).

[3]R. Blatt and G. Werth, Phys. Rev. A **25**, 1476 (1982); R. Blatt, H. Schnatz, and G. Werth, Phys. Rev. Lett. **48**, 1601 (1982); M. D. McGuire, R. Petsch, and G. Werth, Phys. Rev. A **17**, 1999 (1978).

[4]R. Schneider and G. Werth, Z. Phys. A **293**, 103 (1979).

[5]G. Meisel, Verh. Dtsch. Phys. Ges. **22**, A13.1 (1987); **23**, A11.1 (1988).

[6]H. Dehmelt, Adv. At. Mol. Phys. **3**, 53 (1967).

[7]W. Neuhauser, M. Hohenstatt, P. E. Toschek, and H. Dehmelt, Phys. Rev. A **22**, 1137 (1980).

[8]Ch. Gerz, Th. Hilberath, and G. Werth, Z. Phys. D **5**, 97 (1987); Ch. Gerz, J. Roths, F. Vedel, and G. Werth, *ibid.* **8**, 235 (1988); A. Roth and G. Werth, *ibid.* **9**, 265 (1988).

[9]R. F. Wuerker, H. Shelton, and R. V. Langmuir, J. Appl. Phys. **30**, 342 (1959).

[10]E. Fischer, Z. Phys. **156**, 1 (1959).

[11]R. Blatt, P. Zoller, G. Holzmüller, and I. Siemers, Z. Phys. D **4**, 121 (1986).

[12]I. Siemers, R. Blatt, Th. Sauter, and W. Neuhauser, Phys. Rev. A **38**, 5121 (1988).

[13]T. Hänsch, R. Keil, A. Schabert, Ch. Schmelzer, and P. E. Toschek, Z. Phys. **226**, 293 (1969); T. Hänsch and P. E. Toschek, Ann. Phys. (Leipzig) **23**, 271 (1969); G. Orriols, Nuovo Cimento **53B**, 1 (1979).

[14]W. Demtröder, in *Laser Spectroscopy,* Vol. 5 of *Chemical Physics,* edited by Y. I. Goldanskii (Springer, Berlin, 1981); T. Hänsch and P. E. Toschek, IEEE J. Quantum Electron **4**, 467 (1968); Phys. Lett. **20**, 273 (1966).

[15]H. Risken, in *The Fokker-Planck Equation,* Vol. 18 of *Springer Series in Synergetics,* edited by H. Haken (Springer-Verlag, Berlin, 1983).

[16]J. Javanainen, in *Fundamentals of Laser Interactions,* Vol. 229 of *Lecture Notes in Physics,* edited by F. Ehlotzky (Springer, Berlin, 1985), pp. 249–258.

[17]M. H. Prior and R. D. Knight, Opt. Commun. **35**, 54 (1980).